Gain-assisted critical coupling for high-performance coherent perfect absorbers

Jae Woong Yoon, Myoung Jin Jung, and Seok Ho Song*

Department of Physics, Hanyang University, Seoul 133-791, South Korea
**Corresponding author: shsong@hanyang.ac.kr*

Received April 1, 2015; revised April 22, 2015; accepted April 23, 2015;
posted April 23, 2015 (Doc. ID 237351); published May 8, 2015

Balanced radiation and absorption rates of an optical resonator are necessary for coherent perfect light absorption in many active device applications. This balance is referred to as critical coupling condition. We propose a gain-assisted method for exact access to critical coupling conditions without altering any structure parameters. In a coherent absorber with additional internal gain media, critical coupling with arbitrarily high coherent signal extinction can be obtained by continuously tuning optical pumping density. Assuming a surface-plasmon resonance grating covered by a gain layer as a promising architecture, we numerically demonstrate gain-assisted continuous access to its critical coupling point with experimentally probable settings. In addition, the gain tuning further introduces switching of the coherent-absorber's functionality to a conventional lossless beam splitter. © 2015 Optical Society of America

OCIS codes: (030.1670) Coherent optical effects; (240.6680) Surface plasmons; (300.1030) Absorption.
http://dx.doi.org/10.1364/OL.40.002309

Principles of currently developing nanophotonic and plasmonic devices necessarily involve efficient trapping of optical fields in subwavelength scales. Recently, a plausible method of strong light confinement was proposed on the basis of an inverse laser concept called coherent perfect absorption (CPA) [1,2]. Corresponding to the time reversal of laser emission processes, coherent incoming optical fields in a CPA system are completely trapped into a resonance mode producing a null outgoing field due to destructive interference between the different coupling pathways. This coherent trapping effect is highly controllable with phase differences between the multiple incoming fields, providing ultrafast and low-power schemes for optical modulators, switches, and coherence filters [3].

In pursuit of practical device applications, various CPA configurations have been suggested and experimentally demonstrated using surface-plasmonic resonance gratings [4,5], metamaterial absorbers [3,6], graphene monolayers with appropriate patterns, and additional resonant photonic thin-films [7,8]. By exploiting the CPA effect for all-optical active elements in photonic integrated circuit platforms, Bruck and Muskens theoretically investigated silicon-on-insulator waveguide systems loaded with plasmonic nanoantennas [9]. Baum *et al.* recently proposed a parity-time symmetric double plasmonic nanocavity structure [10].

As coherence filters, all-optical modulators, and switches, the performance of CPA devices is fundamentally determined by how closely devices are tuned to an exact critical coupling condition at which the operating resonance mode interacts with a given coupling configuration to yield identical radiation and dissipation rates. Coherent signal extinction ratio is given by $(\gamma_{\mathrm{rad}}-\gamma_{\mathrm{int}})^2/(\gamma_{\mathrm{rad}}+\gamma_{\mathrm{int}})^2$ [4], where γ_{rad} and γ_{int} are the radiation and internal decay rates of a resonance mode, respectively. Therefore, strictly perfect signal extinction can be achieved with the vanishing difference $\gamma_{\mathrm{rad}}-\gamma_{\mathrm{int}}$ at critical coupling conditions. Device tuning for exact critical coupling generally involves careful parametric optimization with time-consuming rigorous numerical simulations. In practice, even a precisely designed device may be subject to off-tuned, poor performance due to fabrication imperfections, unavoidable rough surfaces, and microscopic material properties that differ from bulk optical properties generally used for numerical modeling in parametric optimization.

In this Letter, we propose a gain-assisted critical coupling that is precisely accessible without altering its geometrical parameters. Assuming a surface-plasmonic CPA element including optical gain medium as an exemplary device architecture, we show that appropriate gain tuning in the resonance region provides an efficient method for strictly obtaining coherent perfect absorption. In addition, gain tuning further introduces active switching of device functionality between a CPA element and a conventional lossless beam splitter.

The surface-plasmon-resonance grating structure consists of, from bottom to top, a periodically corrugated Si surface, conformal Ag and SiO_2 films, and a dye-doped PMMA over-layer as shown in Fig. 1(a). The structure is designed so that an SPP mode at the Ag-SiO_2 interface couples to two external plane waves at a desired wavelength. Figure 1(b) illustrates two incoming waves with amplitudes a_1 and a_2 simultaneously coupling with a single SPP mode at different diffraction orders. This coupling configuration produces two outgoing waves

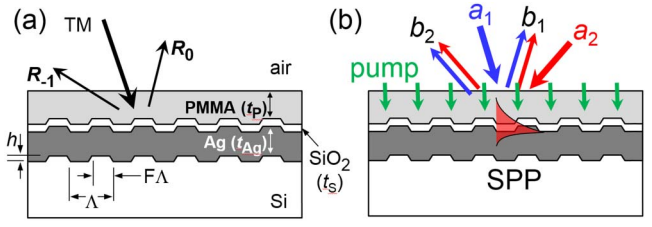

Fig. 1. (a) Schematic of surface-plasmonic CPA element consisting of Si grating and conformal grating layers of Ag, SiO_2 spacer, and dye-doped PMMA as gain medium. (b) Coupling of two input plane wave components (a_1 and a_2) to single SPP mode at Ag-SiO_2 interface. b_1 and b_2 denote amplitudes of two outgoing waves.

with respective amplitudes b_1 and b_2. At critical coupling, where γ_{rad} and γ_{int} of the SPP mode are identical [4,5], outgoing waves b_1 and b_2 simultaneously vanish as a result of complete destructive interference between the balanced resonant and nonresonant diffraction pathways.

General aspects of coherent absorbers are revealed in the temporal coupled-mode theory of a dissipative resonator. Applying the temporal coupled-mode theory of dissipative resonators [4] to the coupling configuration in Fig. 1(b), the net absorbance at the resonance center is expressed by the following formula:

$$A_{net} = \frac{4\gamma_{int}\gamma_{rad}}{(\gamma_{rad}+\gamma_{int})^2}\frac{c_1 I_1 + c_2 I_2 + 2\sqrt{c_1 c_2 I_1 I_2}\cos\phi}{I_1 + I_2}, \quad (1)$$

where $I_n = |a_n|^2$ is incoming power at radiation port n, and ϕ is phase difference in the excited resonance mode separately excited by a_1 and a_2. The relative coupling strength constant c_n is a fractional radiation decay rate of the resonance mode into port n and normalized such that $c_1 + c_2 = 1$. We notice in this general formula that the coherent *perfect* absorption, i.e., $A_{net} = 1$, is obtained at $\phi = 0$ (or integer multiple of 2π) only if $\gamma_{rad} = \gamma_{int}$ and $I_1 : I_2 = c_1 : c_2$. The first condition is referred to as critical coupling condition as mentioned previously. The latter is a condition on relative intensities of the two incoming waves. In contrast to this intensity condition that is subject to an external preparation in experiments, the critical coupling condition can be satisfied only by tuning intrinsic properties of a resonator.

Considering the critical coupling condition in the proposed structure shown in Fig. 1, the radiation decay rate γ_{rad} of the SPP mode are primarily determined by the real part of the dielectric constant and geometrical parameters such as period Λ, grating depth h, and fill-factor F. Therefore, γ_{rad} is fixed for a given structure in practice. In contrast, factors dominantly determining the internal decay rate γ_{int} are ohmic damping of free electrons in Ag film and optical gain in the adjacent dielectric media, i.e., $\gamma_{int} = \gamma_{ohm} - \gamma_{gain}$, where γ_{ohm} and γ_{gain} are partial rates of ohmic dissipation and stimulated amplification of an SPP mode, respectively. These quantities are highly tunable with temperature and pumping energy density. Therefore, the critical coupling condition can be obtained more precisely with optical gain adjustment without modifying geometrical parameters.

For the geometry of interest in Fig. 1, internal decay rate of the SPP is approximated by

$$\gamma_{int} = \gamma_{ohm} - \gamma_{gain} \approx \omega\frac{n^2}{\varepsilon'^2_{Ag}}\varepsilon''_{Ag} - \frac{c}{n}G, \quad (2)$$

where ε'_{Ag} and ε''_{Ag} are real and imaginary dielectric constants of Ag, respectively, ω is angular frequency of incident light, c is speed of light in vacuum, n is refractive index of PMMA, and G is gain coefficient in the PMMA over-layer. Note that the dielectric constant of dye-doped PMMA is given by $\varepsilon = 2.25 + i\varepsilon''$ with $\varepsilon'' = -nG\lambda/2\pi$. Equation (2) is implied in the well-known relation $k_{SP} = (\omega/c)[\varepsilon\cdot\varepsilon_{Ag}/(\varepsilon+\varepsilon_{Ag})]^{-1/2}$ for an in-plane wave vector of the surface plasmon mode on flat surfaces [11]. Notably, γ_{int} is significantly modified for G near or larger than $n^3\varepsilon''_{Ag}\omega/(c\varepsilon'^2_{Ag}) \approx 1.3\times10^3$ cm^{-1}, where γ_{gain} becomes comparable to or larger than γ_{ohm}. This level of optical gain is obtainable with probable experimental settings. Using Rhodamine 6 G dye at a doping concentration of 150 mM as an example, the host PMMA layer has optical gain in a range of $G = -0.9 \sim 3.4\times10^3$ cm^{-1} at emission wavelength 632.8 nm for pumping intensity range of 0–1 MW/cm^2 at 532 nm. In this estimation, we use a gain model suggested in [12] with parameters given in [13] for emission properties of Rhodamine 6 G dye.

We numerically demonstrate the gain-assisted critical coupling in an optimized surface-plasmon-resonance grating structure. Figure 2 shows the gain-dependent absorbance spectrum of an optimized structure under single-plane-wave incidence. Geometrical parameters of the optimized structure are given in the figure caption. The Chandezon method is used for numerical calculation [14]. Si, Ag, and SiO_2 are modeled with their frequency-dependent optical constants listed in Ref. [15].

The gain-dependent absorbance spectra in Fig. 2 show strong resonance peaks at two incidence angles $\theta = 12.5°$ and $-43.5°$ where a single SPP mode is excited through the first- and second-order diffraction processes, respectively. The resonant peaks change bandwidth and peak value depending on the gain coefficient G in the PMMA layer. Angular bandwidth of the absorbance peak decreases with increasing optical gain, as generally expected. Interestingly, peak absorbance does not simply decrease with increasing optical gain. The absorbance peak for $G = 529$ cm^{-1} is slightly higher than the peak for $G = 0$ (no optical gain), as clearly shown in the inset of Fig. 2. The peak absorbance does not simply increase with losses in the resonance region. This unusual effect originates from gain-assisted critical coupling between the SPP mode and external plane waves. Light absorption in a resonant cavity is maximized when the optical field is maximally confined at the critical coupling condition $\gamma_{int} = \gamma_{rad}$. If a given resonance system is under-coupled ($\gamma_{int} > \gamma_{rad}$) in the absence of optical gain, resonant absorption increases as γ_{int} approaches γ_{rad} with increasing optical gain. We note in Fig. 2 that the device is optimized so that the SPP resonance is slightly under-coupled.

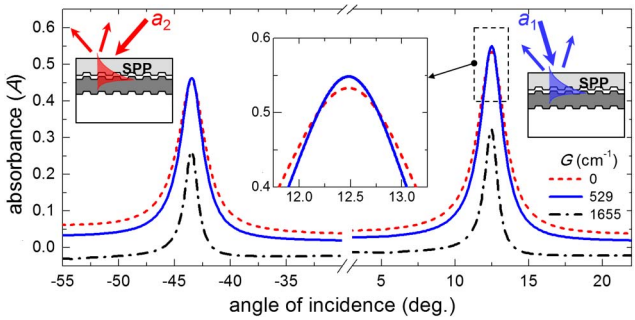

Fig. 2. Angular absorbance spectra at wavelength $\lambda = 632.8$ nm for passive ($G = 0$) and two gain-assisted cases ($G = 529$ and 1655 cm^{-1}). Geometrical parameters of calculated optimal device are $\Lambda = 700$ nm, $F = 0.3$, $h = 30$ nm, $t_{Ag} = 200$ nm, $t_S = 10$ nm, and $t_P = 200$ nm. Inset graph shows magnified absorbance peaks for PMMA gain coefficient $G = 529$ cm^{-1} and 1655 cm^{-1}.

Resonant absorption with two coherent incident waves changes more drastically with optical gain. The response under two-coherent-wave incidence is obtained using a scattering matrix approach with the following equation:

$$\begin{bmatrix} b_1 \\ b_2 \end{bmatrix} = \begin{bmatrix} S_{11} & S_{12} \\ S_{21} & S_{22} \end{bmatrix} \begin{bmatrix} a_1 \\ a_2 \end{bmatrix}. \tag{3}$$

The scattering matrix element S_{pq} is given by diffraction amplitude at the outgoing wave channel b_p under unit-amplitude incidence at the incoming channel a_q. Once scattering matrix elements are found, net outgoing power relative to total incoming power is given by $P_{\text{tot}}/I_{\text{tot}} = \Sigma_p |\Sigma_q S_{pq} a_q|^2 / \Sigma_p |a_p|^2$. Figure 3 shows relative net outgoing power versus gain coefficient G. It shows two coherent cases where SPPs separately excited by a_1 and a_2 build up (in-phase case) and cancel (out-of-phase case) each other. In contrast to an out-of-phase case where the resonant absorption is negligible regardless of the amount of gain, net outgoing power in the in-phase case vanishes at optical gain $G = G_1 = 708.28\ \text{cm}^{-1}$. Therefore, the in-phase case demonstrates gain-assisted coherent perfect absorption. Another interesting point is found at $G = G_2 = 1985.8\ \text{cm}^{-1}$ where in-phase and out-of-phase cases make no difference in the net outgoing power as SPP resonance becomes lossless ($\gamma_{\text{gain}} = \gamma_{\text{ohm}}$ and $\gamma_{\text{int}} = 0$). For higher gain coefficient $G > G_2$, the device enters an amplifying regime where the internal decay rate γ_{int} of the SPP mode becomes negative. Outgoing waves are amplified for the in-phase case with maximal SPP excitation, resulting in higher outgoing power than the out-of-phase case.

Phase-dependent responses at these two particular gain coefficients G_1 and G_2 reveal a clear contrast in device operation as a coherent perfect absorber and conventional lossless beam splitter. At $G = G_1$ for the coherent perfect absorber functionality, outgoing powers $P_1 = |b_1|^2$ and $P_2 = |b_2|^2$ are simultaneously decreasing and vice versa to create perfect absorption and nearly total diffraction states, as shown in Fig. 4(a). In contrast,

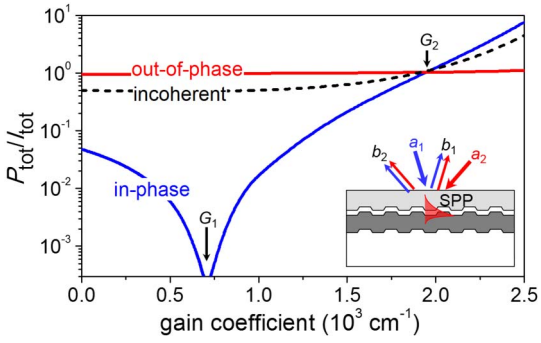

Fig. 3. Comparison between coherent and incoherent responses of normalized total outgoing power with two input waves a_1 at $\theta = 12.5°$ and a_2 at $\theta = -43.5°$ as functions of PMMA gain coefficient. Solid blue and red curves indicate two coherent cases with in-phase and out-of-phase excitations, respectively, while black dotted curve shows incoherent response. In all cases, relative incoming powers are fixed at $|a_1|^2 : |a_2|^2 = 0.54 : 0.46$, following the incoming intensity condition required for the strongest resonance excitation [4,5].

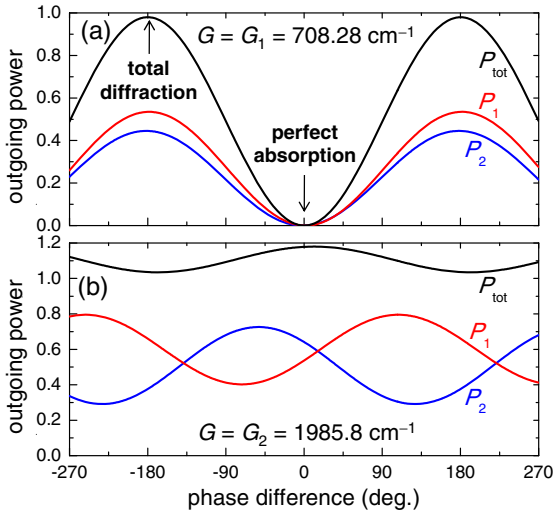

Fig. 4. Phase-sensitive responses of outgoing powers $P_1 = |b_1|^2$ $P_2 = |b_2|^2$, and $P_{\text{tot}} = P_1 + P_2$ for (a) gain-assisted critical coupling at $G = 708.28\ \text{cm}^{-1}$ and (b) gain-assisted lossless resonance at $G = 1985.8\ \text{cm}^{-1}$.

the device at $G = G_2$ shown in Fig. 4(b) acts as a conventional beam splitter where P_1 and P_2 are anti-correlated such that one is decreasing while the other is increasing. Therefore, the gain-assisted coherent absorber can switch its function between a coherent perfect absorber and a conventional beam splitter depending on the optical gain effective to the operating resonance mode.

In conclusion, we propose gain-assisted critical coupling for precise tuning of CPA devices. A surface-plasmon-resonance grating over-coated with gain medium is selected as an example device structure. Rigorous numerical calculation with realistic material properties clearly demonstrates the gain-assisted coherent perfect absorption and nearly lossless total diffraction at exact critical coupling conditions without altering geometrical parameters. In addition, gain tuning further introduces switching of the device functionality to a conventional lossless beam splitter. The proposed gain-tuned coherent absorber scheme can be implemented in various CPA configurations using metamaterial absorbers, graphene nanostructures, and integrated photonic circuit elements to yield high performance at high-speed and low-power operation regimes.

This work was supported in part by the Global Frontier Program through the National Research Foundation of Korea (NRF) funded by the Ministry of Science, ICT & Future Planning (NRF-2014M3A6B3063708).

References

1. Y. D. Chong, L. Ge, H. Cao, and A. D. Stone, Phys. Rev. Lett. **105**, 053901 (2010).
2. W. Wan, Y. Chong, L. Ge, H. Noh, A. D. Stone, and H. Cao, Science **331**, 889 (2011).
3. J. Zhang, K. F. McDonald, and N. I. Zheludev, Light Sci. Appl. **1**, e18 (2012).
4. J. Yoon, K. H. Seol, S. H. Song, and R. Magnusson, Opt. Express **18**, 25702 (2010).
5. J. W. Yoon, G. M. Koh, S. H. Song, and R. Magnusson, Phys. Rev. Lett. **109**, 257402 (2012).

6. S. Feng and K. Halterman, Phys. Rev. B **86**, 165103 (2012).
7. J. Zhang, C. Guo, K. Liu, Z. Zhu, W. Ye, X. Yuan, and S. Qin, Opt. Express **22**, 12524 (2014).
8. J. R. Piper and S. Fan, ACS Photon. **1**, 347 (2014).
9. R. Bruck and O. L. Muskens, Opt. Express **21**, 27652 (2013).
10. B. Baum, H. Alaeian, and J. Dionne, J. Appl. Phys. **117**, 063106 (2015).
11. H. Raether, *Surface Plasmons on Smooth and Rough Surfaces and on Gratings*, Springer Tracks in Modern Physics (Springer-Verlag, 1988), Vol. **111**.
12. I. D. Leon and P. Berini, Opt. Express **17**, 20191 (2009).
13. A. Penzkofer and W. Leupacher, J. Lumines. **37**, 61 (1987).
14. J. Chandezon, M. T. Dupuis, G. Cornet, and D. Maystre, J. Opt. Soc. Am. **72**, 839 (1982).
15. E. D. Palik, *Handbook of Optical Constants of Solids II* (Academic, 1998).